AGU PUBLICATIONS

JGR

Journal of Geophysical Research: Solid Earth

RESEARCH ARTICLE
10.1002/2015JB011980

Key Points:
- Impact of SAL on Earth rotation estimated using surface mass models
- SAL is important for polar motion excitations, especially oceanic excitations
- SAL is not as important for length-of-day excitations but global mass balance is

Correspondence to:
K. J. Quinn,
kquinn@aer.com

Citation:
Quinn, K. J., R. M. Ponte, and M. E. Tamisiea (2015), Impact of self-attraction and loading on Earth rotation, *J. Geophys. Res. Solid Earth*, *120*, 4510–4521, doi:10.1002/2015JB011980.

Received 24 FEB 2015
Accepted 22 MAY 2015
Accepted article online 27 MAY 2015
Published online 19 Jun 2015

Impact of self-attraction and loading on Earth rotation

Katherine J. Quinn[1], Rui M. Ponte[1], and Mark E. Tamisiea[2]

[1] Atmospheric and Environmental Research, Lexington, Massachusetts, USA, [2] National Oceanography Centre, Liverpool, UK

Abstract The impact of self-attraction and loading (SAL) on Earth rotation has not been previously considered except at annual timescales. We estimate Earth rotation excitations using models of atmospheric, oceanic, and land hydrology surface mass variations and investigate the importance of including SAL over monthly to interannual timescales. We assess SAL effects in comparison with simple mass balance effects where net mass exchanged with the atmosphere and land is distributed uniformly over the global ocean. For oceanic polar motion excitations, SAL impacts are important even though mass balance impact is minor except at the annual period. This is true of global (atmosphere + land + ocean) polar motion excitations as well, although the SAL impacts are smaller. When estimating length-of-day excitations, mass balance effects have a dominant impact, particularly for oceanic excitation. Although SAL can have a significant impact on estimated Earth rotation excitations, its consideration generally did not improve comparisons with geodetic observations. This result may change in the future as surface mass models and Earth rotation observations improve.

1. Introduction

The Earth's hydrologic system is constantly redistributing and exchanging mass within and between its components. These mass variations induce changes in the Earth's rotation, as described by the Earth orientation parameters of polar motion and length-of-day (LOD) [*Barnes et al.*, 1983]. Models of the hydrologic system components, i.e., atmosphere, oceans, and land hydrology, can be used to estimate the forced rotational variations.

The interactions between the Earth's hydrologic system components must be gravitationally consistent. Nonuniform surface mass variations will induce changes in the gravity field and surface deformation [*Farrell and Clark*, 1976; *Blewitt and Clarke*, 2003], sometimes called the self-attraction and loading (SAL) effect, which will result in nonuniform changes to nonsteric sea surface height and associated ocean bottom pressure. The SAL effects of the individual system components can be separately examined, as in *Tamisiea et al.* [2010] and *Vinogradova et al.* [2010, 2011]. These SAL changes in ocean bottom pressure will naturally lead to changes in Earth rotation. However, we know of only one study of low-degree gravity harmonics [*Clarke et al.*, 2005] that includes SAL effects and indicates that for annual periods the effects can be significant for the degree 2 harmonics that relate directly to Earth rotation.

The SAL formulation in these studies implicitly conserves mass of the individual components (and therefore the total system) by exchanging net mass with the ocean component. However, it is important to note that SAL effects are active even when there are no such net mass transfers; i.e., mass is merely redistributed within each component. It is thus useful to split SAL contributions over the ocean into two components: (1) a net mass balance component that is defined by distributing any net mass exchanged with the atmosphere and land uniformly over the global ocean, which does not involve any modeling of SAL effects, and (2) the residual spatially variable component, which captures the most relevant SAL physics. Most studies of oceanic Earth rotation excitations ignore both (1) and (2) components [e.g., *Ponte and Stammer*, 1999; *Nastula and Salstein*, 1999; *Johnson et al.*, 1999; *Ponte and Stammer*, 2000; *Ponte et al.*, 2001; *Chen et al.*, 2004, 2005; *Yan et al.*, 2006]. Studies that also include excitations from land hydrology tend to account only for (1) [e.g., *Chen*, 2005; *Dobslaw et al.*, 2010; *Yan and Chao*, 2012].

Going beyond Earth rotation, properly considering SAL may also be important for estimating and interpreting observations of any geodetic measurement affected by surface mass variations. *Clarke et al.* [2005] noted that implementing SAL has a significant impact on geocenter estimates at annual periods and also affects higher degree components of the gravity field. *Tamisiea et al.* [2010] estimated SAL impacts on sea level at annual

periods and noted improved comparisons with tide gauge data. *Vinogradova et al.* [2010, 2011] considered SAL effects on ocean bottom pressure at annual, subannual, and interannual time scales and showed that including SAL generally improved comparisons with in situ bottom pressure recorders and Gravity Recovery and Climate Experiment (GRACE) observations. Examples of other observing systems that will be affected by SAL are satellite gravimeters, satellite laser ranging, in situ gravimeters, satellite altimeters, Global Navigation Satellite Systems (GNSS), and Very Long Baseline Interferometry (VLBI).

In this work, we estimate Earth rotation excitations using models of atmospheric, oceanic, and hydrological surface loads and investigate the importance of the SAL effect over monthly to interannual timescales. In the context of previous papers on the subject, we assess SAL effects in comparison with a simplified mass balance model using the simple uniform layer assumption described above. In section 2, we give a brief overview of the SAL formulation and the Earth rotation excitation equations. Section 3 describes the geophysical fluid models and the geodetic data used to compare with the models. Results are presented and discussed in sections 4 and 5. The goal of this paper is to show for which Earth rotation components and for which timescales SAL is important and at what level, in relation to simple effects of net mass balance.

2. Theory

2.1. Self-Attraction and Loading

The SAL methodology is as described in *Tamisiea et al.* [2010], and we will only summarize the main points here. Loading in regions with additional mass results in a locally depressed crust and uplift in the surrounding regions. Mass changes from the loading have a corresponding gravity field change that produces a small gravitational force away from the local depression. There is also a direct gravitational attraction toward the local mass anomaly. All these effects combine to produce an increased gravitational force toward mass anomalies in the near field and a decreased force farther away. The resulting nonuniform sea surface height variations are estimated by solving the sea level equation [*Farrell and Clark*, 1976] using an iterative pseudospectral approach [*Mitrovica and Peltier*, 1991]. As in previous works [*Rietbroek et al.*, 2011; *Jensen et al.*, 2013], we include the sea level changes due to rotational feedback of the SAL mass redistribution [*Wu and Peltier*, 1984; *Milne and Mitrovica*, 1998]. This formulation is valid for timescales longer than the Chandler wobble (~14 months) [*Mitrovica et al.*, 2005]. At shorter periods, no equivalent formulation is available. The sensitivity of our results to the exclusion of rotational feedback is discussed in section 4. The SAL adjustments to surface mass anomalies are assumed to be static; i.e., they cause no dynamic variations in the ocean, which is plausible at monthly and longer timescales [*Kuhlmann et al.*, 2011; *Vinogradova et al.*, 2015]. The Earth deformation is assumed to be elastic, which is reasonable for less than decadal timescales. For a given surface mass distribution from atmospheric, oceanic, and/or hydrological models, this methodology can be used to estimate a gravitationally self-consistent spatially variable sea level field, accounting along the way for conservation of total mass in the system.

2.2. Earth Rotation Excitation

Earth rotation excitations are forced by surface mass distribution changes and motion changes (e.g., winds and ocean currents). This study focuses on the mass excitations, which can be computed as follows [*Eubanks*, 1993]:

$$\chi_1 = -\frac{1.098R^4}{C-A}\int\int \Delta\sigma(\phi,\lambda)\sin\phi\cos^2\phi\cos\lambda \mathrm{d}\lambda\mathrm{d}\phi \tag{1}$$

$$\chi_2 = -\frac{1.098R^4}{C-A}\int\int \Delta\sigma(\phi,\lambda)\sin\phi\cos^2\phi\sin\lambda \mathrm{d}\lambda\mathrm{d}\phi \tag{2}$$

$$\chi_3 = \frac{0.753R^4}{C_m}\int\int \Delta\sigma(\phi,\lambda)\cos^3\phi \mathrm{d}\lambda\mathrm{d}\phi \tag{3}$$

where χ_1 and χ_2 are the two components of polar motion excitation, χ_3 is the LOD excitation, ϕ and λ are latitude and longitude, R is the Earth's mean radius (6.371×10^6m), A and C are the Earth's principle moments of inertia ($C - A = 2.61 \times 10^{35}\,\mathrm{kg\,m^2}$), C_m is the mantle's principle moment of inertia ($7.1236 \times 10^{37}\,\mathrm{kg\,m^2}$), $\Delta\sigma$ is the time variable surface mass density (units of $\mathrm{kg\,m^{-2}}$). The effective excitation functions ($\chi_{\{1,2,3\}}$) are dimensionless quantities.

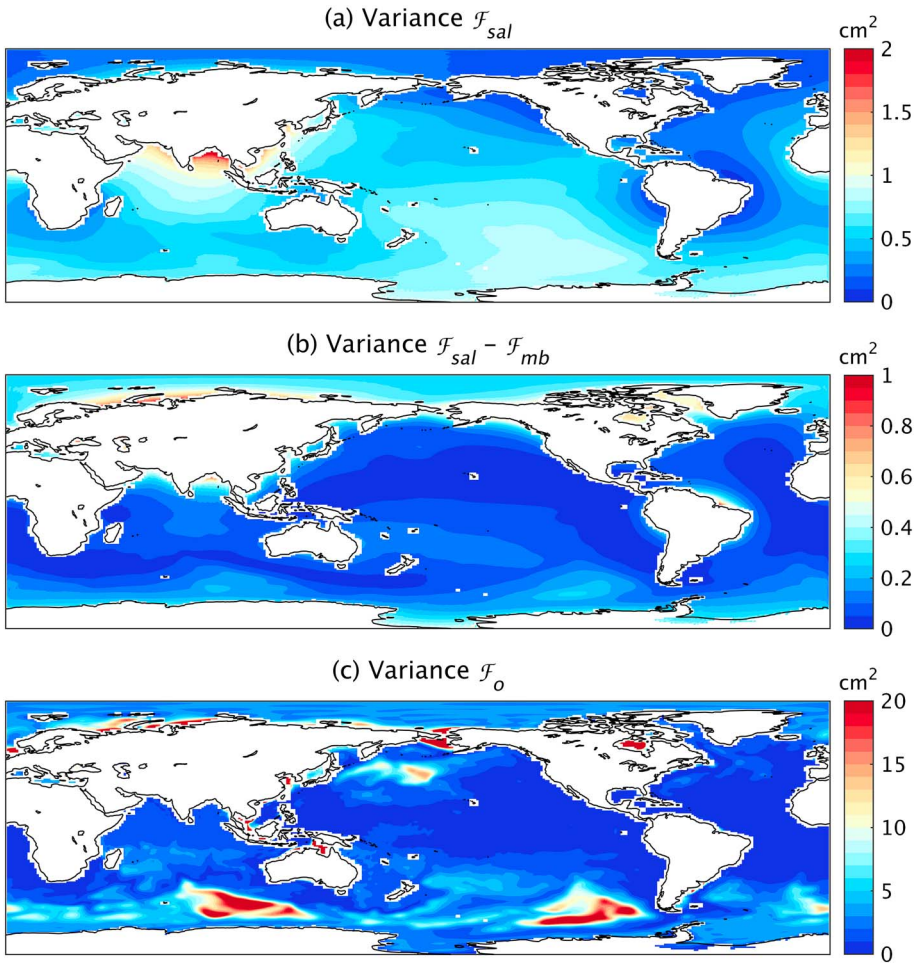

Figure 1. Variance of (a) SAL-induced surface mass load ($\mathcal{F}_{sal}$), (b) $\mathcal{F}_{sal}$ minus its spatial mean ($\mathcal{F}_{sal} - \mathcal{F}_{mb}$), and (c) dynamic ocean mass ($\mathcal{F}_o$). Units are cm^2 of equivalent water height. All data have been detrended.

3. Data

3.1. Surface Mass Models

Our analysis considers monthly time series for the 11 year period from 2003 to 2013, for which Gravity Recovery and Climate Experiment (GRACE) data and the respective atmospheric and oceanic dealiasing products (AOD1B) are available [*Dobslaw et al.*, 2013; *Flechtner et al.*, 2014]. We use Release-05 GRACE and AOD1B data.

The atmospheric pressure in AOD1B is taken from the European Center for Medium-Range Weather Forecasts (ECMWF) operational analyses (http://www.ecmwf.int/research/ifsdocs/index.html). At monthly periods the ocean tends to respond as an inverted barometer to surface atmospheric pressure changes [e.g., *Ponte*, 1992]; therefore, for the purposes of surface loading the atmospheric pressure over the entire ocean is taken as a uniform value equal to the mean pressure over the ocean.

The ocean mass variability in AOD1B is taken from the Ocean Model for Circulation and Tides (OMCT) [*Thomas et al.*, 2001]. The OMCT setup for GRACE is forced with wind stresses, 2 m temperatures, atmospheric freshwater fluxes, and surface pressure from the ECMWF operational analyses. For this setup, dynamic SAL feedbacks are not incorporated. The model does not assimilate altimetry, which minimizes the chance that SAL effects will be erroneously incorporated into the model. The ocean model uses a Boussinesq formulation, i.e., conserves volume rather than mass. To remove spurious mass changes, we subtract from the bottom pressure fields a uniform equivalent water layer equal to the spatial mean bottom pressure [*Greatbatch*, 1994; *Ponte*, 1999]. We denote the resulting bottom pressure anomalies as the dynamic ocean mass variability, i.e., generated by ocean dynamics and not by mass transfer from the land or atmosphere. In order to describe the total

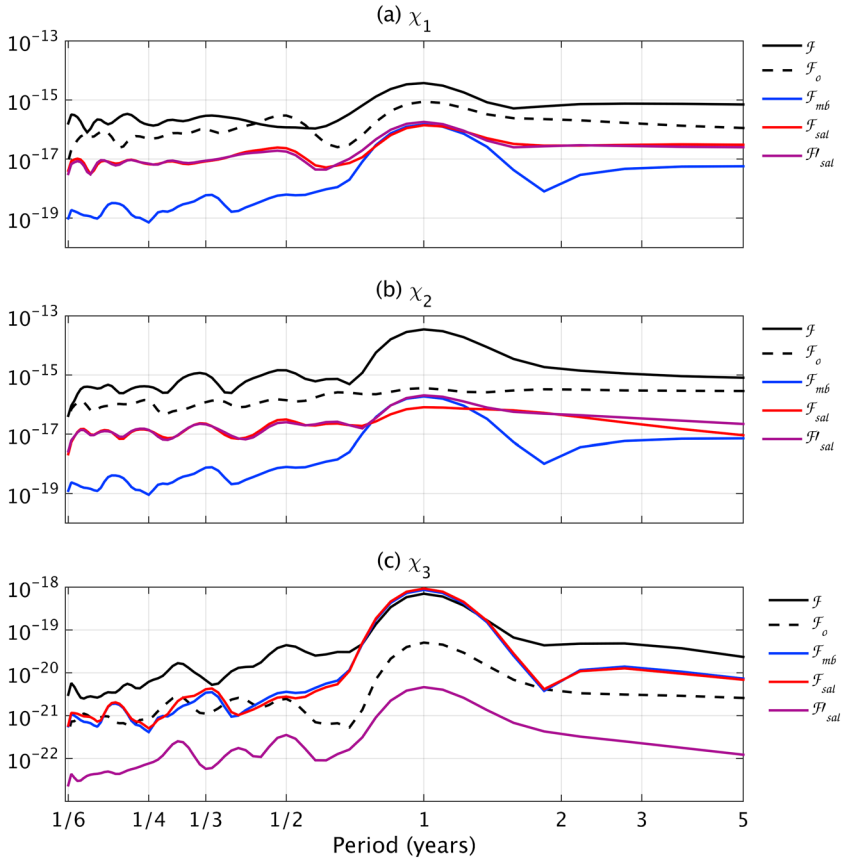

Figure 2. Spectra of Earth rotation excitations: (a) χ_1, (b) χ_2, and (c) χ_3. $\mathcal{F}$ = atmosphere + dynamic ocean + land hydrology forcing, $\mathcal{F}_o$ = dynamic ocean-only forcing, $\mathcal{F}_{mb}$ = uniform mass conservation forcing, $\mathcal{F}_{sal}$ = SAL forcing, $\mathcal{F}'_{sal}$ = SAL minus uniform mass conservation. Units are dimensionless measures of angular momentum squared per (cycle/yr). Spectra estimated using Welch's method as implemented in the MATLAB function pwelch.

ocean variability, we will need to add either a spatially uniform mass that balances land and atmosphere mass variability or add SAL variability as described in section 2.

The continental hydrology variability is derived from the GRACE Release-05 land mass grids [*Landerer and Swenson*, 2012; *Swenson and Wahr*, 2006]. We use an equally weighted ensemble mean of the solutions produced by the three main processing centers of GFZ (GeoForschungsZentrum Potsdam), CSR (Center for Space Research, University of Texas), and JPL (Jet Propulsion Laboratory). Using an ensemble mean solution tends to reduce noise in the GRACE data [*Sakumura et al.*, 2014]. These data include surface mass variations over Greenland and Antarctica that are caused by changing ice masses.

3.2. Geodetic Observations

The observed daily polar motion and LOD excitations are from the International Earth Rotation and Reference System (IERS) combined time series (C04) with tidal variations removed. The LOD excitation is directly proportional to the observed LOD. The polar motion excitations are computed from observed pole coordinates via the method described in *Vicente and Wilson* [2002] using a Chandler quality factor of 175 and period of 433 days. These daily observed Earth rotation excitations are averaged into monthly mean values.

To compare with the modeled excitations (estimated using equations (1)–(3) and the surface mass models), we must remove the motion (winds and ocean currents) excitations from the observed geodetic excitations. The winds and ocean currents are from the same models that were used to estimate the surface mass loads, i.e., ECMWF and OMCT. The motion excitations were generated at the German Research Centre for Geosciences (https://www.gfz-potsdam.de/en/section/earthsystemmodelling/services/eam/). We note that a majority of the variability in LOD is due to atmospheric winds.

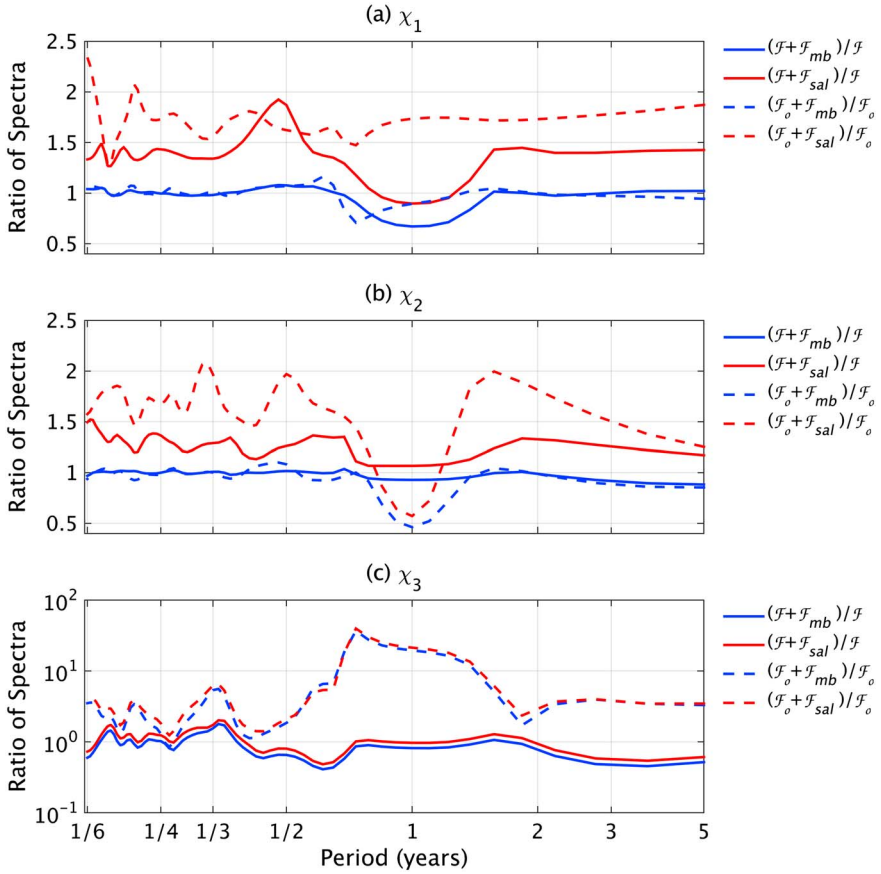

Figure 3. Ratios of power spectra of Earth rotation excitations: (a) χ_1, (b) χ_2, and (c) χ_3. $\mathcal{F}$ = atmosphere + dynamic ocean + land hydrology forcing, $\mathcal{F}_o$ = dynamic ocean-only forcing, $\mathcal{F}_{mb}$ = mass conservation forcing, $\mathcal{F}_{sal}$ = SAL forcing.

Much of the trends in Earth rotation are assumed to be due to postglacial rebound; therefore, we detrend all our modeled surface mass fields and derived excitations as well as the observed excitations. The data are detrended by a joint least squares estimation of trend, annual, and semiannual variability. Also, the observed LOD has a prominent 6 year cycle and decadal variations that are due to core-mantle interactions [*Holme and*

Table 1. Subannual (Period < 12 Months) and Interannual (Detrended, Period > 18 Months; 18 Months < Period < 5 Years for LOD) Excitations: Comparisons of Oceanic and Total Excitations With and Without SAL or Uniform Mass Balance[a]

	χ_1				χ_2				χ_3	
	%change		Correlations		%change		Correlations		%change	Correlations
					Subannual					
$\mathcal{F}_o + \mathcal{F}_{sal}$ versus $\mathcal{F}_o$	67	(47)	0.99	(1.00)	70	(50)	0.99	(1.00)	132	0.67
$\mathcal{F}_o + \mathcal{F}_{mb}$ versus $\mathcal{F}_o$	3		1.00		−1		1.00		93	0.58
$\mathcal{F} + \mathcal{F}_{sal}$ versus $\mathcal{F}$	37	(20)	1.00		28	(14)	1.00		−10	0.92
$\mathcal{F} + \mathcal{F}_{mb}$ versus $\mathcal{F}$	1		1.00		1		1.00		−26	0.92
					Interannual					
$\mathcal{F}_o + \mathcal{F}_{sal}$ versus $\mathcal{F}_o$	63		0.97		48		0.99		290	0.19
$\mathcal{F}_o + \mathcal{F}_{mb}$ versus $\mathcal{F}_o$	−7		0.98		−11		0.99		282	−0.09
$\mathcal{F} + \mathcal{F}_{sal}$ versus $\mathcal{F}$	41		1.00		25		1.00		−38	0.76
$\mathcal{F} + \mathcal{F}_{mb}$ versus $\mathcal{F}$	0		1.00		−7		1.00		−48	0.77

[a]Values in brackets are for SAL with no rotational feedback, shown only where differences occur. %change is percent change in variance.

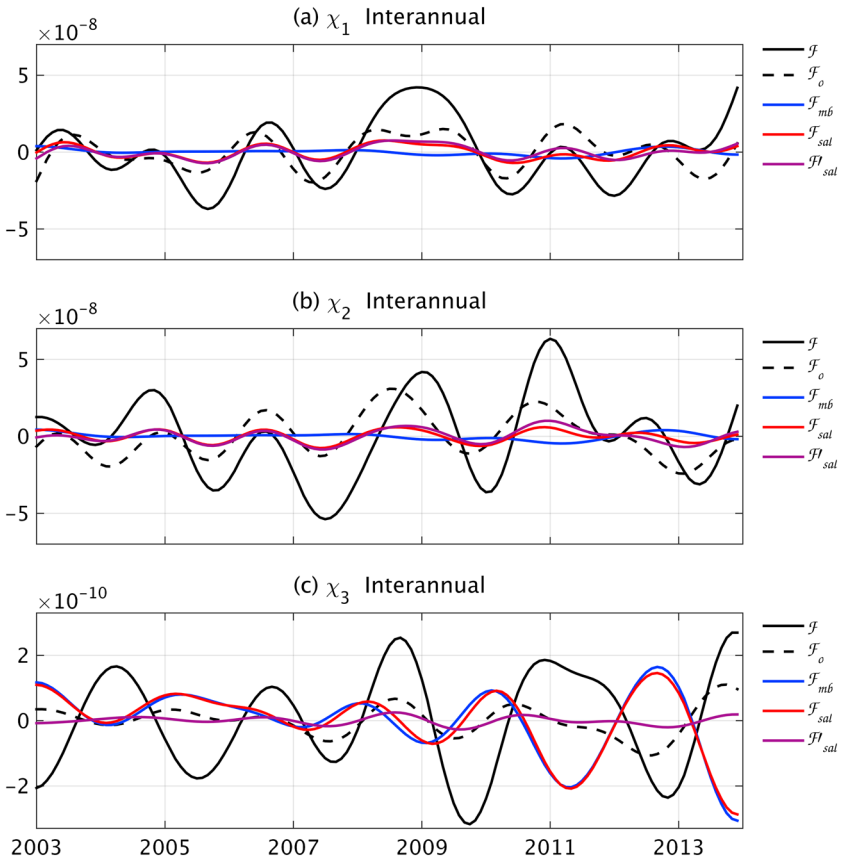

Figure 4. Earth rotation excitations for interannual periods (detrended, more than 18 months): (a) χ_1, (b) χ_2, and (c) χ_3. $\mathcal{F}$ = atmosphere + dynamic ocean + land hydrology forcing, $\mathcal{F}_o$ = dynamic ocean-only forcing, $\mathcal{F}_{\mathrm{mb}}$ = mass conservation forcing, $\mathcal{F}_{\mathrm{sal}}$ = SAL forcing, $\mathcal{F}'_{\mathrm{sal}}$ = SAL minus uniform mass conservation. Units are dimensionless angular momentum.

de Viron, 2013]. We high-pass filter all our modeled and observed LOD excitation time series with a cutoff period of 5 years using a Butterworth filter, so as to only investigate excitations due to surface mass variability. In the following sections the observed geodetic excitations are denoted as $\mathcal{G}$ and respective mass components as $\mathcal{G}_{\mathrm{mass}}$.

Table 2. Annual Excitations: Modeled Excitations With and Without SAL or Uniform Mass Balance and Comparisons to Geodetic Excitations

	χ_1		χ_2		χ_3	
	A[a] ($\times 10^{-8}$)	ϕ[b] (°)	A ($\times 10^{-8}$)	ϕ (°)	A ($\times 10^{-10}$)	ϕ (°)
$\mathcal{F}_o$	2.3 ± 0.6	70 ± 14	1.4 ± 0.7	33 ± 27	2.0 ± 0.3	254 ± 7
$\mathcal{F}_o + \mathcal{F}_{\mathrm{mb}}$	2.3 ± 0.6	95 ± 14	0.9 ± 0.7	87 ± 43	8.5 ± 0.4	189 ± 3
$\mathcal{F}_o + \mathcal{F}_{\mathrm{sal}}$	3.1 ± 0.7	82 ± 14	1.0 ± 0.9	6 ± 52	8.9 ± 0.4	192 ± 3
$\mathcal{F}$	4.5 ± 1.0	345 ± 13	16 ± 2	298 ± 6	7.1 ± 0.7	304 ± 6
$\mathcal{F} + \mathcal{F}_{\mathrm{mb}}$	3.5 ± 1.0	342 ± 16	15 ± 2	295 ± 6	6.6 ± 0.6	234 ± 6
$\mathcal{F} + \mathcal{F}_{\mathrm{sal}}$	4.0 ± 1.2	356 ± 17	16 ± 2	297 ± 6	7.2 ± 0.7	235 ± 15
$\mathcal{G}_{\mathrm{mass}}$	4.7 ± 1.3	312 ± 15	15 ± 2	312 ± 7	3.4 ± 1.0	241 ± 15
$\mathcal{G}_{\mathrm{mass}} - \mathcal{F}$	2.6 ± 1.0	241 ± 21	3.8 ± 1.1	51 ± 16	6.4 ± 0.8	155 ± 7
$\mathcal{G}_{\mathrm{mass}} - (\mathcal{F} + \mathcal{F}_{\mathrm{mb}})$	2.4 ± 0.9	264 ± 23	4.6 ± 1.1	39 ± 14	3.0 ± 0.7	46 ± 14
$\mathcal{G}_{\mathrm{mass}} - (\mathcal{F} + \mathcal{F}_{\mathrm{sal}})$	3.3 ± 1.0	255 ± 17	4.5 ± 1.1	55 ± 14	3.6 ± 0.7	48 ± 12

[a] Amplitude, units are dimensionless angular momentum.
[b] Phase, referenced to 1 January 2005.

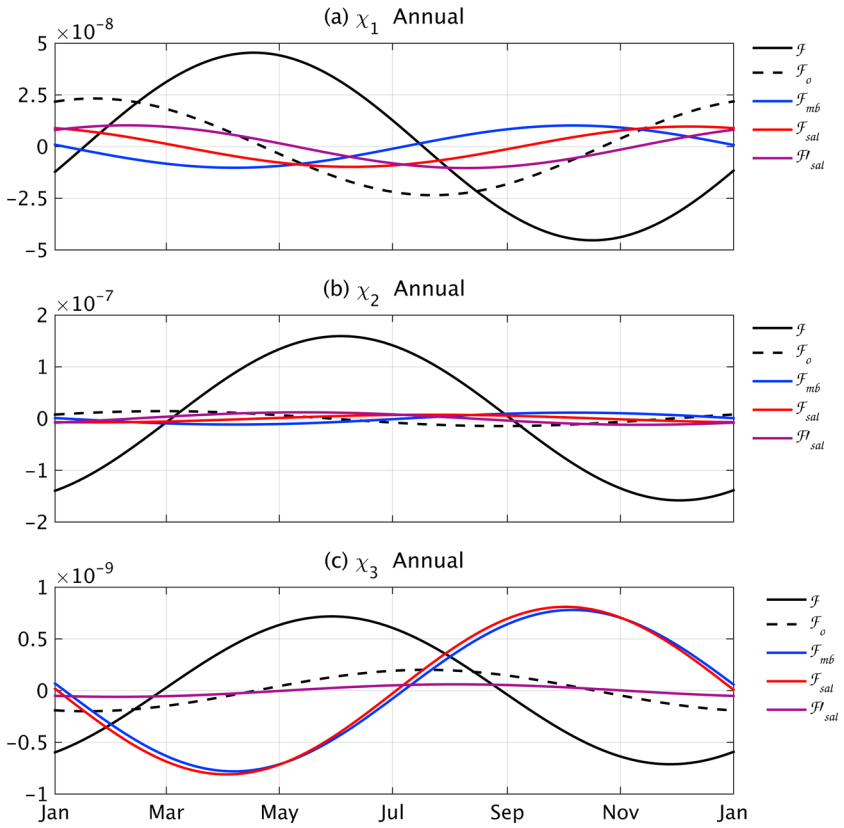

Figure 5. Earth rotation excitations for annual period: (a) χ_1, (b) χ_2, and (c) χ_3. $\mathcal{F}$ = atmosphere + dynamic ocean + land hydrology forcing, $\mathcal{F}_o$ = dynamic ocean-only forcing, $\mathcal{F}_{mb}$ = mass conservation forcing, $\mathcal{F}_{sal}$ = SAL forcing, $\mathcal{F}'_{sal}$ = SAL minus uniform mass conservation. Units are dimensionless angular momentum.

3.3. Surface Mass Combinations and Notations

In the subsequent sections of this paper, we combine the surface mass models in various ways to assess the impact of SAL on the estimation of the Earth rotation excitation series in (1)–(3). Here we provide notations to define these combinations. Mass variations resulting from ocean dynamics only, i.e., the output from OMCT with the Greatbatch correction (as described above), will be denoted as $\mathcal{F}_o$. To $\mathcal{F}_o$, we add mass variations from the atmosphere and land hydrology to describe the total surface mass forcing *before* the inclusion of any implicit mass transfers to the ocean and SAL effects, which will be denoted as $\mathcal{F}$. Separate consideration of overall mass balance using a uniform distribution over the oceans will be denoted by $\mathcal{F}_{mb}$. A main comparison will be with $\mathcal{F}_{sal}$, which includes both mass variations due to SAL effects and to net mass exchanges with the ocean. Therefore, with mass balanced and conserved for the Earth system of ocean + atmosphere + land hydrology, mass variations over the ocean without SAL effects are $\mathcal{F}_o + \mathcal{F}_{mb}$ and with SAL effects are $\mathcal{F}_o + \mathcal{F}_{sal}$. Surface mass variations over the whole Earth without SAL effects are $\mathcal{F} + \mathcal{F}_{mb}$ and with SAL effects are $\mathcal{F} + \mathcal{F}_{sal}$. Deviations of $\mathcal{F}_{sal}$ from $\mathcal{F}_{mb}$, i.e., $\mathcal{F}_{sal} - \mathcal{F}_{mb}$, are denoted as $\mathcal{F}'_{sal}$.

4. Results

The variance of detrended SAL-induced ocean mass changes ($\mathcal{F}_{sal}$) is shown in Figure 1a. Values range from a high of 2 cm^2 in the Bay of Bengal to a low of 0.2 cm^2 at high northern latitudes and coastal regions around South America. Figure 1b shows the detrended SAL variance with a spatial mean removed at each time step (i.e., $\mathcal{F}'_{sal}$). Values range from close to zero in midlatitudes up to 0.8 cm^2 near the coasts, particularly at high latitudes. The spatially uniform net mass balance component of detrended SAL (i.e., $\mathcal{F}_{mb}$) has a variance of approximately 0.4 cm^2. The reduced variance between Figures 1a and 1b indicates that net mass balance is a large component of $\mathcal{F}_{sal}$. The spatial pattern of $\mathcal{F}_{mb}$ is simply the ocean portion of the land/ocean mask.

For comparison to $\mathcal{F}_{sal}$ and $\mathcal{F}_{mb}$, Figure 1c shows the variance of the dynamic ocean mass variations, $\mathcal{F}_o$, which does not include any net mass change effects. The values are highest (>20 cm^2) for shallow continental shelf

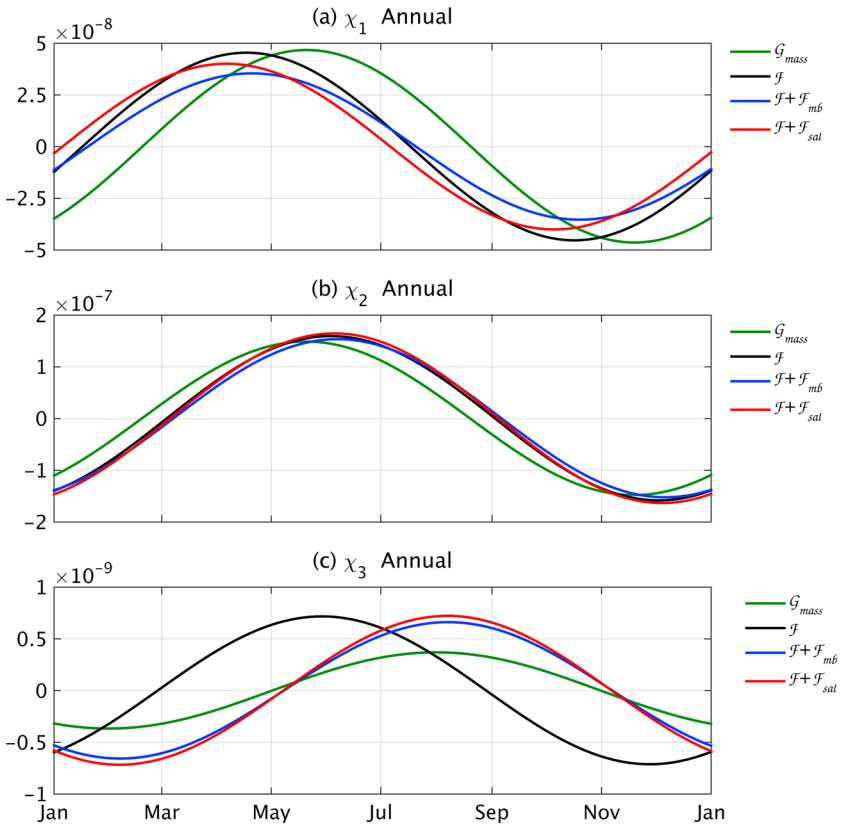

Figure 6. Earth rotation excitations for annual period: (a) χ_1, (b) χ_2, and (c) χ_3. $\mathcal{G}_{\text{mass}}$ = geodetic observations, $\mathcal{F}$ = atmosphere + dynamic ocean + land hydrology forcing, $\mathcal{F}_{\text{mb}}$ = mass conservation forcing, $\mathcal{F}_{\text{sal}}$ = SAL forcing. Units are dimensionless angular momentum.

regions, and there is also high variability in the Southern Ocean (10–20 cm^2) and a small region of the North Pacific (10 cm^2). In general, the variance in $\mathcal{F}_o$ is much higher than that in $\mathcal{F}_{\text{sal}}$ or $\mathcal{F}_{\text{mb}}$, except for areas of weak oceanic variability such as the low and middle latitudes. Treatment of SAL effects thus seems important for accurate representation of bottom pressure variability at low latitudes. For example, a study by *Piecuch* [2013] in the tropical Pacific noted discrepancies between GRACE bottom pressure observations (which implicitly include SAL) and estimates from a simple ocean model. Some of the mismatch may be due to neglecting SAL physics in the model. The relative importance of SAL at low latitudes has also been used to demonstrate the ability of equatorial bottom pressure recorders to recover the annual ocean mass change [*Hughes et al.*, 2012; *Williams et al.*, 2014].

Using the surface mass variations shown in Figure 1 as well as the atmospheric and hydrological models described in section 3, we estimated the forced Earth rotation excitations. We show the spectra for the separate components in Figure 2. For polar motion and LOD, the relative power of the excitations are similar except at the annual period; therefore, we will discuss nonannual and annual periods separately. As stated in section 3, the annual cycle is determined with a joint least squares estimation of the trend, annual, and semi-annual variations. For subannual variability we use a 12 month high-pass Butterworth filter applied to data with the trend and annual cycle removed. Interannual variability is determined using a 18 month low-pass Butterworth filter applied to detrended data.

For polar motion at nonannual frequencies, the variance of excitations due to $\mathcal{F}_{\text{mb}}$ is much lower than that due to $\mathcal{F}_{\text{sal}}$ or $\mathcal{F}'_{\text{sal}}$, which is lower than either $\mathcal{F}_o$ or $\mathcal{F}$ (Figures 2a and 2b). This indicates that $\mathcal{F}_{\text{mb}}$ should have less impact on polar motion excitation than $\mathcal{F}_{\text{sal}}$; therefore, $\mathcal{F}_{\text{mb}}$ will not be a good approximation for $\mathcal{F}_{\text{sal}}$ when estimating polar motion. This can be seen more clearly in Figures 3a and 3b, which have the variance ratios of the total global excitations with SAL or uniform mass balance ($\mathcal{F}+\mathcal{F}_{\text{sal}}$ or $\mathcal{F}+\mathcal{F}_{\text{mb}}$) to $\mathcal{F}$ and the variance ratios of the total ocean excitations with SAL or uniform mass balance ($\mathcal{F}_o+\mathcal{F}_{\text{sal}}$ or $\mathcal{F}_o+\mathcal{F}_{\text{mb}}$) to $\mathcal{F}_o$. The excitation variance ratios with $\mathcal{F}_{\text{mb}}$ (Figures 3a and 3b, blue lines) are ~1 at nonannual periods whereas the ratios with $\mathcal{F}_{\text{sal}}$

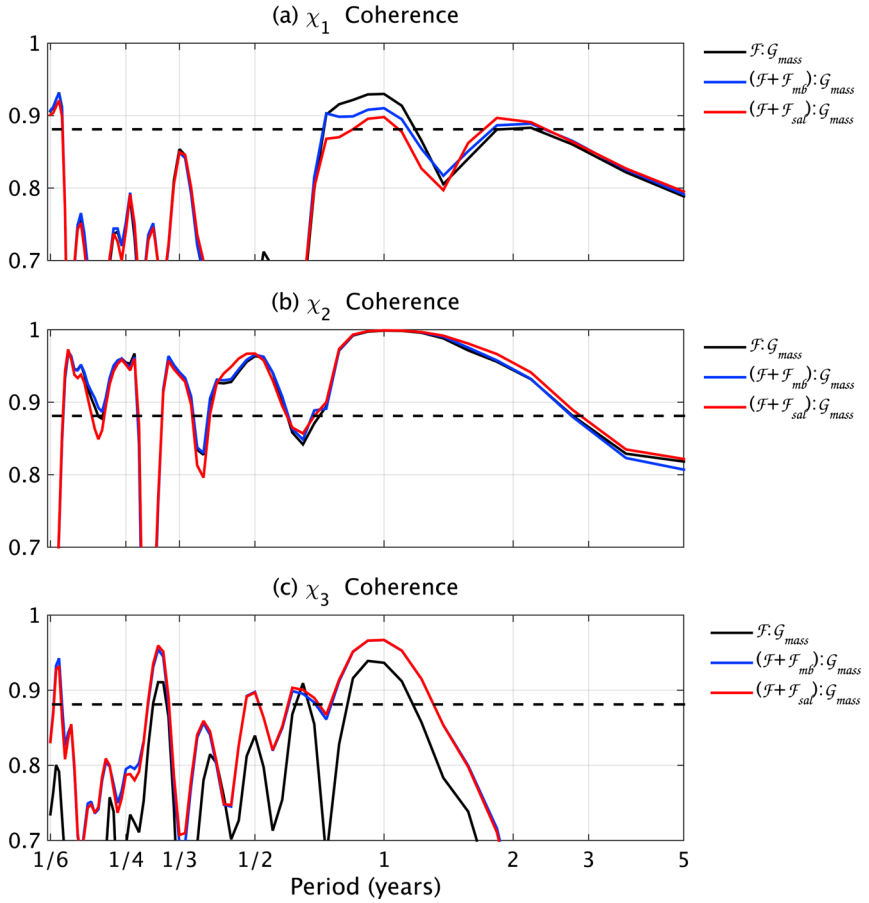

Figure 7. Amplitude of coherence of modeled Earth rotation excitations with geodetic observations: (a) χ_1, (b) χ_2, and (c) χ_3. $\mathcal{G}_{\text{mass}}$ = geodetic observations, $\mathcal{F}$ = atmosphere + dynamic ocean + land hydrology forcing, $\mathcal{F}_{\text{mb}}$ = uniform mass conservation forcing, $\mathcal{F}_{\text{sal}}$ = SAL forcing. Coherence estimated using Welch's method as implemented in the MATLAB function mscohere.

(Figures 3a and 3b, red lines) are considerably higher. These percent variance changes averaged for subannual (less than 12 months) and interannual (detrended, more than 18 months) periods are listed in Table 1. For SAL impacts with respect to $\mathcal{F}_o$, the excitation variance changes range from 48% to 70%, and with respect to $\mathcal{F}$ the excitation variance changes range from 25% to 41%. Figure 4 shows the time series of excitations filtered to show only interannual periods. As already stated, for polar motion the variability forced by $\mathcal{F}_{\text{mb}}$ is relatively small but that forced by $\mathcal{F}_{\text{sal}}$ is larger, particularly for χ_1 (see also the percent changes in variance in Table 1). However, as in Table 1, note that the impact of SAL is smaller for global than for ocean polar motion excitation estimates for nonannual periods because $\mathcal{F}$ is significantly larger than $\mathcal{F}_o$.

For LOD excitations at nonannual periods, the excitation variances forced by $\mathcal{F}_{\text{mb}}$ and $\mathcal{F}_{\text{sal}}$ are very similar and $\mathcal{F}'_{\text{sal}}$ is comparatively very small (Figure 2c), indicating that the net mass balance component dominates the total SAL effect for these estimates. When estimating the total ocean excitation ($\mathcal{F}_o+\mathcal{F}_{\text{sal}}$ or $\mathcal{F}_o+\mathcal{F}_{\text{mb}}$), including at least the net mass balance effects is very important. As seen in Table 1, the LOD excitation variance due to $\mathcal{F}_o+\mathcal{F}_{\text{sal}}$ or $\mathcal{F}_o+\mathcal{F}_{\text{mb}}$ is approximately 2 (3) times higher for subannual (interannual) periods than that due to $\mathcal{F}_o$ alone. However, since $\mathcal{F}_o$ effects on LOD excitation are small compared to $\mathcal{F}$ (Figure 2c), the impact of $\mathcal{F}_{\text{mb}}$ or $\mathcal{F}_{\text{sal}}$ on the total global excitation is much smaller (~30–50% variance change for $\mathcal{F}_{\text{mb}}$ or ~10–40% for $\mathcal{F}_{\text{sal}}$, Table 1). This is illustrated at interannual periods in Figure 4c. We note that the patterns for LOD excitations are also quite different, leading to the lower correlations seen in Table 1, whereas for polar motion the patterns are similar and correlations close to one. In Figure 4c, LOD excitations forced by $\mathcal{F}$ and $\mathcal{F}_{\text{mb}}$ (or $\mathcal{F}_{\text{sal}}$) are actually anticorrelated and tend to cancel each other out, as can be seen in the negative changes in variance in Table 1. This relationship is largely due to land hydrology exchanges with the ocean having impacts of opposite sign in LOD, noted previously in *Chen* [2005].

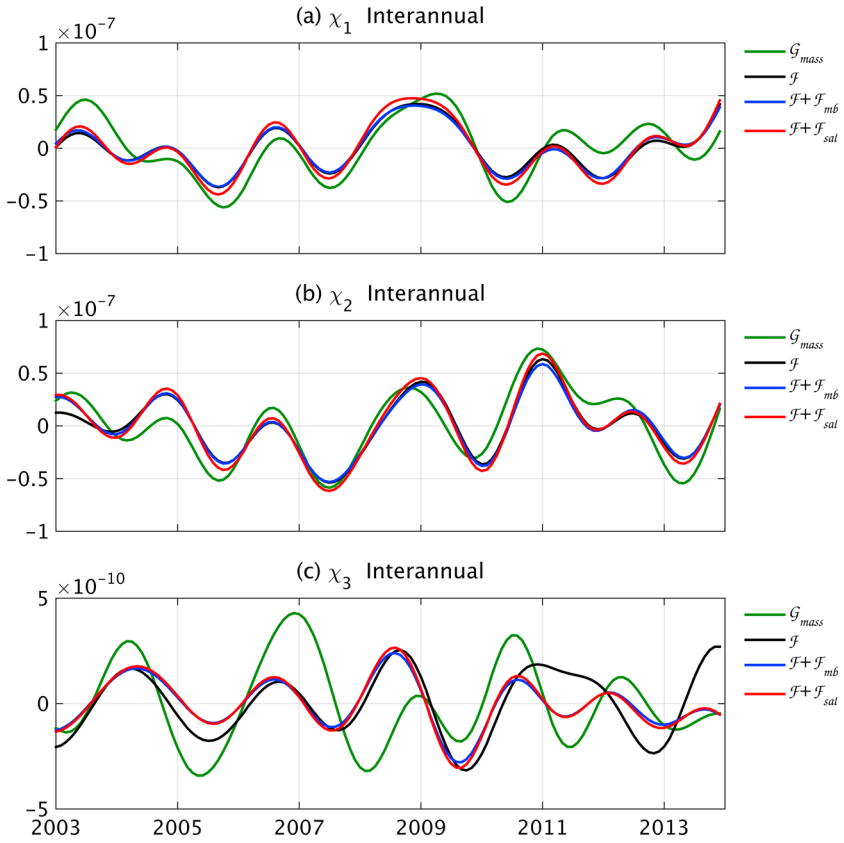

Figure 8. Earth rotation excitations for interannual periods (detrended, more than 18 months): (a) χ_1, (b) χ_2, and (c) χ_3. $\mathcal{G}_{\text{mass}}$ = geodetic observations, $\mathcal{F}$ = atmosphere + dynamic ocean + land hydrology forcing, $\mathcal{F}_{\text{mb}}$ = mass conservation forcing, $\mathcal{F}_{\text{sal}}$ = SAL forcing. Units are dimensionless angular momentum.

Behavior at annual periods is distinct from other periods for both polar motion and LOD excitations. For oceanic polar motion excitations (forced by $\mathcal{F}_o$, $\mathcal{F}_o + \mathcal{F}_{\text{sal}}$, or $\mathcal{F}_o + \mathcal{F}_{\text{mb}}$) the amplitudes and phases are all quite different (Table 2; Figures 5a and 5b). For global polar motion excitations, $\mathcal{F}$ is much larger than $\mathcal{F}_{\text{sal}}$ or $\mathcal{F}_{\text{mb}}$ (Figures 5a and 5b); therefore, adding these effects will not significantly change the estimates (Figures 6a and 6b).

For annual LOD excitations, $\mathcal{F}_o$ forcing is small compared to the other terms; therefore, including $\mathcal{F}_{\text{sal}}$ or $\mathcal{F}_{\text{mb}}$ in the forcing makes a big difference and essentially dominates the total oceanic excitation estimate (Figure 3c and Table 2). Similar to subannual and interannual periods, the variability in net mass transfers captured in $\mathcal{F}_{\text{mb}}$ contributes strongly to that in $\mathcal{F}_{\text{sal}}$. Global LOD excitations forced by $\mathcal{F}$ and $\mathcal{F}_{\text{sal}}$ (or $\mathcal{F}_{\text{mb}}$) have similar amplitudes but different phases (Figure 5c); therefore, including $\mathcal{F}_{\text{sal}}$ or $\mathcal{F}_{\text{mb}}$ will have a significant impact on the phase (Table 2 and Figure 6c).

We have seen that $\mathcal{F}_{\text{sal}}$ can have a significant impact on the oceanic and total Earth rotation excitations, depending on the timescale and rotation component. We now consider whether $\mathcal{F}_{\text{sal}}$ can improve modeled estimates of excitations compared to the mass component of observed geodetic excitations ($\mathcal{G}_{\text{mass}}$). We calculated the coherence between global polar motion excitations with and without SAL and observed mass excitations (Figure 7). For χ_1 there is significant coherence (at the 95% confidence level) between modeled and observed excitations (Figure 7a) only for annual and biennial periods. For χ_2 there is significant coherence at subannual, annual, and longer periods (see also Figures 6b and 8b). At interannual periods, χ_2 excitations forced by $\mathcal{F} + \mathcal{F}_{\text{sal}}$ have slightly higher coherence than those forced by $\mathcal{F} + \mathcal{F}_{\text{mb}}$ or $\mathcal{F}$ alone. Annual χ_1 and χ_2 excitations forced by $\mathcal{F} + \mathcal{F}_{\text{sal}}$ do not have statistically significant differences to those forced by $\mathcal{F} + \mathcal{F}_{\text{mb}}$ or $\mathcal{F}$ alone (Table 2).

For LOD, the coherence between the modeled mass excitations and the observed mass excitations is improved across all time scales by adding $\mathcal{F}_{\text{sal}}$ (or $\mathcal{F}_{\text{mb}}$) to $\mathcal{F}$ (see also Figures 6c and 8c). Whereas LOD excitations due to

$\mathcal{F} + \mathcal{F}_{sal}$ (or $\mathcal{F} + \mathcal{F}_{mb}$) are coherent for all time scales, $\mathcal{F}$ yields significant coherence only for annual and some subannual time scales. However, excitations due to $\mathcal{F}$ and $\mathcal{G}_{mass}$ are significantly out of phase at the annual period (Figure 6c and Table 2).

As mentioned in section 2.1, given that the use of rotational feedback in SAL estimates at periods less than 14 months remains an open issue, we recalculated all our results without including rotational feedback in SAL in order to assess its impact. In this case, the general result is a reduction in SAL impact for polar motion only: the percent variance changes are somewhat reduced at subannual timescales (see Table 1). There are, however, no significant changes in the annual excitation results discussed in Table 2 and Figures 5 and 6.

5. Discussion and Summary

When modeling total surface mass variations for the Earth system, it is important to be gravitationally consistent and include the SAL effects. We have used models of surface mass variations for the land hydrology, the atmosphere, and the oceans and the induced SAL effects to estimate their impact on Earth rotation excitations. The formulation of SAL effects implicitly accounts for net mass transfers to the ocean. For comparison, we have also considered the relative importance of accounting for net mass exchanges with the ocean by assuming a simple uniform distribution over the global ocean.

For estimating LOD excitations, our results show that one does not gain significantly more information by considering SAL effects in addition to accounting for net mass transfers using a simple uniform layer approximation. Mass balance considerations are, nevertheless, very important, especially when estimating ocean-only LOD excitations at all frequencies and also when estimating global LOD excitations at annual frequencies.

For estimating polar motion excitations, mass balance effects are minor except for annual periods, where they become important but not dominant. For estimating ocean-only polar motion excitation, including SAL effects is very important at all frequencies. For estimating global polar motion excitations, including SAL is moderately important at nonannual periods (changes excitation variance by ~30–40%, Table 1) but plays a relatively minor role at the annual period.

The general rule of thumb is that only net mass balance effects are important for LOD excitation, whereas SAL effects are important for polar motion excitations. Of course, this depends on the frequencies of interest and the level of error one is willing to tolerate in the excitation estimates. Our conclusions are for the most part qualitative since the details of the variances and ratios are dependent on the Earth system models used. However, our main conclusions should be immune to model details. This is corroborated by results we obtained using older data from *Tamisiea et al.* [2010], where we reached the same general conclusions on the impact of SAL. Our results provide important guidelines for assessing modeling errors for Earth rotation excitations when SAL impacts are disregarded.

This paper focused on the impact of SAL on LOD and polar motion. We have shown that the impacts on estimated excitations, particularly for polar motion, can be quite significant. However, consideration of SAL effects did not generally translate into improved comparisons with geodetic observations of Earth rotation. Noise levels in all the time series can be a problem. As surface mass models and Earth rotation observations improve in the future, incorporation of SAL effects will become more important.

Acknowledgments

The data to support this article are available as follows: atmospheric and ocean mass data were obtained from JPL's Physical Oceanography Distributed Active Archive Center (ftp://podaac-ftp.jpl.nasa.gov/allData/grace/L2/GFZ/RL05/); GRACE land data were processed by Sean Swenson, supported by the NASA MEaSUREs Program and are available at http://grace.jpl.nasa.gov; geodetic data available at the IERS Earth Orientation Centre's interactive website on excitation of polar motion and LOD (http://hpiers.obspm.fr/eop-pc/index.php?index=excitactive&lang=en); motion terms of length-of-day and polar motion available at the GFZ Earth Angular Momentum data archive (ftp://ftp.gfz-potsdam.de/pub/home/ig/ops/IERS_opECMWF/). This work was supported by NASA grants NNX14AJ51G, NNX12AJ93G, and NNX11AC14G. Mark Tamisiea was supported through core funding provided by the Natural Environment Research Council to the National Oceanography Centre.

References

Barnes, R. T. H., R. Hide, A. A. White, and C. A. Wilson (1983), Atmospheric angular momentum fluctuations, length-of-day changes and polar motion, *Proc. R. Soc. London, Ser. A*, *387*, 31–73.

Blewitt, G., and P. Clarke (2003), Inversion of Earth's changing shape to weigh sea level in static equilibrium with surface mass redistribution, *J. Geophys. Res.*, *108*(B6), 2311, doi:10.1029/2002JB002290.

Chen, J. (2005), Global mass balance and the length-of-day variation, *J. Geophys. Res.*, *110*, B08404, doi:10.1029/2004JB003474.

Chen, J. L., C. R. Wilson, and B. D. Tapley (2005), Interannual variability of low-degree gravitational change, 1980–2002, *J. Geod.*, *78*, 535–543, doi:10.1007/s00190-004-0417-y.

Chen, J.-L., C. R. Wilson, X.-G. Hu, Y.-H. Zhou, and B. D. Tapley (2004), Oceanic effects on polar motion determined from an ocean model and satellite altimetry: 1993–2001, *J. Geophys. Res.*, *109*, B02411, doi:10.1029/2003JB002664.

Clarke, P. J., D. A. Lavallée, G. Blewitt, T. M. van Dam, and J. M. Wahr (2005), Effect of gravitational consistency and mass conservation on seasonal surface mass loading models, *Geophys. Res. Lett.*, *32*, L08306, doi:10.1029/2005GL022441.

Dobslaw, H., R. Dill, A. Grötzsch, A. Brzezinski, and M. Thomas (2010), Seasonal polar motion excitation from numerical models of atmosphere, ocean, and continental hydrosphere, *J. Geophys. Res.*, *115*, B10406, doi:10.1029/2009JB007127.

Dobslaw, H., F. Flechtner, I. Bergmann-Wolf, C. Dahle, R. Dill, S. Esselborn, I. Sasgen, and M. Thomas (2013), Simulating high-frequency atmosphere-ocean mass variability for de-aliasing of satellite gravity observations: AOD1B RL05, *J. Geophys. Res. Oceans*, *118*, 3704–3711, doi:10.1002/jgrc.20271.

Eubanks, T. M. (1993), Variations in the orientation of the Earth, in *Contributions of Space Geodesy to Geodynamics: Earth Dynamics*, edited by D. E. Smith and D. L. Turcotte, AGU, Washington, D. C.

Farrell, W. E., and J. A. Clark (1976), On postglacial sea level, *Geophys. J. R. Astron. Soc.*, *46*, 647–667.

Flechtner, F., H. Dobslaw, and E. Fagiolini (2014), AOD1B product description document for product release 05 (Rev. 4.2), GRACE 327-750, Deutsches GeoForschungsZentrum, Potsdam, Germany.

Greatbatch, R. J. (1994), A note on the representation of steric sea level in models that conserve volume rather than mass, *J. Geophys. Res.*, *99*, 12,767–12,771.

Holme, R., and O. de Viron (2013), Characterisation and implications of intradecadal variations in length-of-day, *Nature*, *499*, 202–204, doi:10.1038/nature12282.

Hughes, C. W., M. E. Tamisiea, R. J. Bingham, and J. Williams (2012), Weighing the ocean: Using a single mooring to measure changes in the mass of the ocean, *Geophys. Res. Lett.*, *39*, L17602, doi:10.1029/2012GL052935.

Jensen, L., R. Rietbroek, and J. Kusche (2013), Land water contribution to sea level from GRACE and Jason-1 measurements, *J. Geophys. Res. Oceans*, *118*, 212–226, doi:10.1002/jgrc.20058.

Johnson, T. J., C. R. Wilson, and B. F. Chao (1999), Oceanic angular momentum variability estimated from the Parallel Ocean Climate Model, 1988–1998, *J. Geophys. Res.*, *104*(B11), 25,183–25,195, doi:10.1029/1999JB900231.

Kuhlmann, J., H. Dobslaw, and M. Thomas (2011), Improved modeling of sea level patterns by incorporating self-attraction and loading, *J. Geophys. Res.*, *116*, C11036, doi:10.1029/2011JC007399.

Landerer, F. W., and S. C. Swenson (2012), Accuracy of scaled GRACE terrestrial water storage estimates, *Water Resour. Res.*, *48*, W04531, doi:10.1029/2011WR011453.

Milne, G. A., and J. X. Mitrovica (1998), Postglacial sea-level change on a rotating Earth, *Geophys. J. Int.*, *133*, 1–19.

Mitrovica, J. X., and W. R. Peltier (1991), On postglacial geoid subsidence over the equatorial oceans, *J. Geophys. Res.*, *96*, 20,053–20,071.

Mitrovica, J. X., J. Wahr, I. Matsuyama, and A. Paulson (2005), The rotational stability of an ice-age Earth, *Geophys. J. Int.*, *161*, 491–506, doi:10.1111/j.1365-246X.2005.02609.x.

Nastula, J., and D. Salstein (1999), Regional atmospheric angular momentum contributions to polar motion excitation, *J. Geophys. Res.*, *104*(B4), 7347–7358, doi:10.1029/1998JB900077.

Piecuch, C. G. (2013), Dynamics of satellite-derived interannual ocean bottom pressure variability in the western tropical North Pacific, *J. Geophys. Res. Oceans*, *118*, 5117–5128, doi:10.1002/jgrc.20374.

Ponte, R. M. (1992), The sea level response of a stratified ocean to barometric pressure forcing, *J. Phys. Oceanogr.*, *22*, 109–113.

Ponte, R. M. (1999), A preliminary model study of the large-scale seasonal cycle in bottom pressure over the global ocean, *J. Geophys. Res.*, *104*, 1289–1300.

Ponte, R. M., and D. Stammer (1999), Role of ocean currents and bottom pressure variability on seasonal polar motion, *J. Geophys. Res.*, *104*, 23,393–23,410.

Ponte, R. M., and D. Stammer (2000), Global and regional axial ocean angular momentum signals and length-of-day variations (1985–1996), *J. Geophys. Res.*, *105*(C7), 17,161–17,171, doi:10.1029/1999JC000157.

Ponte, R. M., D. Stammer, and C. Wunsch (2001), Improving ocean angular momentum estimates using a model constrained by data, *Geophys. Res. Lett.*, *28*, 1775–1778, doi:10.1029/2000GL011671.

Rietbroek, R., S.-E. Brunnabend, J. Kusche, and J. Schrter (2011), Resolving sea level contributions by identifying fingerprints in time-variable gravity and altimetry, *J. Geodyn.*, *59-60*, 72–81, doi:10.1016/j.jog.2011.06.007.

Sakumura, C., S. Bettadpur, and S. Bruinsma (2014), Ensemble prediction and intercomparison analysis of GRACE time-variable gravity field models, *Geophys. Res. Lett.*, *41*, 1389–1397, doi:10.1002/2013GL058632.

Swenson, S. C., and J. Wahr (2006), Post-processing removal of correlated errors in GRACE data, *Geophys. Res. Lett.*, *33*, L08402, doi:10.1029/2005GL025285.

Tamisiea, M. E., E. M. Hill, R. M. Ponte, J. L. Davis, I. Velicogna, and N. T. Vinogradova (2010), Impact of self-attraction and loading on the annual cycle in sea level, *J. Geophys. Res.*, *115*, C07004, doi:10.1029/2009JC005687.

Thomas, M., J. Sündermann, and E. Maier-Reimer (2001), Consideration of ocean tides in an OGCM and impacts on subseasonal to decadal polar motion excitation, *Geophys. Res. Lett.*, *28*(12), 2457–2460.

Vicente, R., and C. Wilson (2002), On long-period polar motion, *J. Geod.*, *76*(4), 199–208.

Vinogradova, N. T., R. M. Ponte, M. E. Tamisiea, J. L. Davis, and E. M. Hill (2010), Effects of self-attraction and loading on annual variations of ocean bottom pressure, *J. Geophys. Res.*, *115*, C06025, doi:10.1029/2009JC005783.

Vinogradova, N. T., R. M. Ponte, M. E. Tamisiea, K. J. Quinn, E. M. Hill, and J. L. Davis (2011), Self-attraction and loading effects on ocean mass redistribution at monthly and longer time scales, *J. Geophys. Res.*, *116*, C08041, doi:10.1029/2011JC007037.

Vinogradova, N. T., R. M. Ponte, K. J. Quinn, M. E. Tamisiea, J.-M. Campin, and J. L. Davis (2015), Dynamic adjustment of the ocean circulation to self-attraction and loading effects, *J. Phys. Oceanogr.*, *45*, 678–689, doi:10.1175/JPO-D-14-0150.1.

Williams, J., C. W. Hughes, M. E. Tamisiea, and S. D. P. Williams (2014), Weighing the ocean with bottom-pressure sensors: Robustness of the ocean mass annual cycle estimate, *Ocean Sci.*, *10*, 701–718, doi:10.5194/os-10-701-2014.

Wu, P., and W. R. Peltier (1984), Pleistocene deglaciation and the Earth's rotation: A new analysis, *Geophys. J. R. Astron. Soc.*, *76*, 753–791.

Yan, H., M. Zhong, Y. Zhu, L. Liu, and X. Cao (2006), Nontidal oceanic contribution to length-of-day changes estimated from two ocean models during 1992–2001, *J. Geophys. Res.*, *111*, B02410, doi:10.1029/2004JB003538.

Yan, H., and B. F. Chao (2012), Effect of global mass conservation among geophysical fluids on the seasonal length of day variation, *J. Geophys. Res.*, *117*, B02401, doi:10.1029/2011JB008788.